BJR

https://doi.org/10.1259/bjr.20200321

Received: 02 April 2020 | Revised: 17 June 2020 | Accepted: 22 June 2020

Cite this article as:
Conficoni A, Feraco P, Mazzatenta D, Zoli M, Asioli S, Zenesini C, et al. Biomarkers of pituitary macroadenomas aggressive behaviour: a conventional MRI and DWI 3T study. *Br J Radiol* 2020; **93**: 20200321.

FULL PAPER

Biomarkers of pituitary macroadenomas aggressive behaviour: a conventional MRI and DWI 3T study

[1,2]ALBERTO CONFICONI, MD, [3,4]PAOLA FERACO, MD, [5]DIEGO MAZZATENTA, MD, [5]MATTEO ZOLI, MD, [6]SOFIA ASIOLI, MD, [7]CORRADO ZENESINI, [3,6]VISCARDO PAOLO FABBRI, MD, [2]MARTINO CELLERINI, MD and [2]ANTONELLA BACCI, MD

[1]Department of Radiology, Neuroradiology Unit, Azienda Ospedaliero-Universitaria di Ferrara, Via Aldo Moro, 44124 Ferrara, Italy
[2]Department of Neuroradiology, Ospedale Bellaria, IRCCS Institute of Neurological Sciences of Bologna, Via Altura, 3; 40100 Bolgona, Italy
[3]Department of Experimental, Diagnostic and Specialty Medicine (DIMES), University of Bologna, Via S. Giacomo 14, 40138 Bologna, Italy
[4]Department of Neuroradiology, Ospedale S. Chiara, Azienda Provinciale per i Servizi Sanitari, Largo medaglie d'oro 9, 38122 , Trento, Italy
[5]Department of Biomedical and Neuromotor Sciences (DIBINEM) of Neurological Sciences of Bologna, Pituitary Unit, Center for the Diagnosis and Treatment of Hypothalamic and Pituitary Diseases, Bologna, Italy
[6]Section of Anatomic Pathology 'M. Malpighi', Bellaria Hospital, Bologna, Italy, Via Altura9; 40100 Bolgona, Italy
[7]Epidemiology and Statistics Unit, IRCCS Istituto delle Scienze Neurologiche di Bologna, Bologna, Italy

Address correspondence to: Dr Paola Feraco
E-mail: *paolaferaco@yahoo.it;paola.feraco@apss.tn.it*

Objective: Pituitary macroadenomas (PAs) are usually defined as benign intracranial tumors. However, they may present local aggressive course. High Ki67 labelling index (LI) values have been related to an aggressive tumor behavior. A recent clinicopathological classification of PA based on local invasiveness and proliferation indexes, divided them in groups with different prognosis. We evaluated the utility of conventional MRI (cMRI) and diffusion-weighted imaging (DWI), in predicting the Ki67- LI according the clinicopathological classification.
Methods: 17 patients (12 M and 5 F) who underwent surgical removal of a PA were studied. cMRI features, quantification of T_1W and T_2W signal intensity, degree of contrast uptake (enhancement ratio, ER) and apparent diffusion coefficient (ADC) values were evaluated by using a 3 T scan. Statistics included Mann–Whitney test, Spearman's test, and receiver operating characteristic analysis. A value of $p \leq 0.05$ was considered significant for all the tests.
Results: Negative correlations were observed between Ki-67 LI, ADCm (ρ = - 0.67, p value = 0.005) and ER values (ρ = −0.62; p = 0.008). ER values were significantly lower in the proliferative PA group (p = 0.028; p = 0.017). ADCm showed sensitivity and specificity of 90 and 85% respectively into predict Ki67-LI value. A value of ADCm ≤0, 711 x 10–6 mm^2 emerged as a cut-off of a value of Ki67-LI ≥ 3%.
Conclusion: Adding quantitative measures of ADC values to cMRI could be used routinely as a non-invasive marker of specific predictive biomarker of the proliferative activity of PA.
Advances in knowledge: Routinely use of DWI on diagnostic work-up of pituitary adenomas may help in establish the likely biological aggressive lesions.

INTRODUCTION

Pituitary adenomas (PA) are the most common tumor of the sellar region in adults and account for approximately up to 80% of all tumors in this location.They are usually classified as functioning or non-functioning, depending on whether they are responsible for hormonal oversecretion, and they are further categorized as macro- or microadenomas depending on their size.[1]

Despite the typical benign histological appearance, pituitary adenomas may present a vast range of biological behavior, and, in some cases, an aggressive course characterized by rapid growth with gross invasion of the surrounding tissues, together with resistance, or early recurrence, after treatment.[2–5] Establishing the aggressive biological behavior of these lesions is essential for both an appropriate surgical resection and long-term follow-up, especially in presence of a residual lesion after treatment. The 2017 WHO Classification of Tumours of Endocrine Organs[6,7] recommends, together with routine histological and immunohistochemical analysis, the systematic evaluation of the tumor proliferation by the assessment of mitotic count and Ki-67 labelling index (LI). These are essential for defining the biological aggressiveness of a PA, as they are directly associated with the likelihood of relapse.[7]

As well-known, conventional MRI (cMRI) is able to show a combination of anatomic features related to the likelihood of cavernous sinuses invasion by pituitary adenomas.[1,2] However, it does not provide any meaningful information regarding PAs proliferative potential. Among the advanced MR techniques, diffusion-weighted imaging (DWI) exploits the incoherent thermally induced motion of water molecules (Brownian motion) in biological tissues within different compartments (*i.e.* intracellular, extracellular, intravascular and transmembrane). Every pathophysiological process which alters the relationships between these compartments, as well as their composition, will thereby affect the motility of water molecules. These changes can be either visualized by DWI and measured by apparent diffusion coefficient (ADC), allowing this technique to define an architectural organization of biological tissues more accurately than conventional sequences.[8–11]

In particular, a stronger inverse relationship has been described between tumor cellularity and the quantitative value obtained from the ADC parametric maps.[12] Considering the pituitary region, a few studies have explored the potential of DWI to identify pituitary macroadenomas (PM) biological aggressiveness by analyzing the correlation with the Ki67-LI nuclear antigen.[9,13]

An exploration of the role of DWI techniques in the characterization of pituitary tumors could yield useful information. Indeed, the possibility of predicting the Ki-67 LI would allow to select those patients with proliferative adenomas, thus both providing important information regarding the surgical planning and follow-up for untreated patients or those with a macroscopic residual tumor. Moreover, Trouillas et al recently proposed a new classification system based both on local invasiveness criteria assessed by MRI and the use of proliferation criteria (the number of mitoses, Ki-67 LI and protein p53 detection).[2] The study demonstrated that adenomas defined as being "invasive and proliferative" (Grade 2b) had a worse prognosis, with an increased probability of tumor persistence or progression of 25- or 12-fold as compared to "non-invasive" and "non-proliferative" adenomas respectively.

Thus, the aim of our study was to evaluate the utility of cMRI sequences and ADC maps, in predicting the Ki-67 index. We also decided to explore the existence of a possible relationship between the information obtained from MRI and the clincopathological classification proposed by Trouillas et al trying to find an MRI biomarker that allows the characterization of the 2b group (invasive and proliferative).[2]

METHODS AND MATERIALS

Our (*Etic Committee: Area Vasta Centro, Bologna, protocol: PIT-MRI-201*) institution's ethics committee approved the study and all patients gave their written informed consent before having the MRI. Patients undergoing surgical removal of a suspected PM between June and October 2019 were enrolled in the study. Only patients with a histological diagnosis of PM and a report including histopathological and immunohistochemical characteristics in accordance with the fourth Edition (2017) of the WHO Classification of Tumors of Endocrine Organs[6] were then considered. Therefore, 17 patients (12 males and 5 females), with an average age of 56.1 ± 10.0 years at the time of surgery, were recruited.

Imaging protocol

The cMRI studies were performed using a high magnetic field intensity system (3 T – *Magnetom Skyra – Siemens Healthcare, Erlangen, Germany*) with a 64-channel *Head/Neck* coil. The conventional sequences included a targeted study of the pituitary region with high spatial resolution (coronal T_2 weighted turbo spin echo (TSE) and coronal and sagittal T_1 weighted TSE sequences both before and after contrast medium administration) and a whole-brain study (axial T_2 weighted TSE sequences, DWI, T_1 weighted 3D SPACE after contrast agent injection); in order to better evaluate the lateral extent of the tumor and its relationship with the cavernous sinuses, three-dimensional time-of-flight MR angiography technique was performed after contrast medium administration.[14,15] The following elements were evaluated:

-*Size of the lesion*: major diameters (anteroposterior, laterolateral, craniocaudal), volume;

-*Tumor invasiveness*: the tumor was considered "invasive" when it surrounded at least 67% of the circumference of the internal carotid artery,according the Grades 3 or 4 of the Knosp grading system,[15,16] and in all cases of evident invasion of the sphenoid sinus[2] ;

-*Signal intensity (SI) homogeneity*: tumors containing a predominant cystic component exceeding 50% of total tumor volume were considered "macrocystic"; tumors containing a predominant hematic content exceeding 50% of the total tumor volume were considered "macrohemorrhagic"; the presence of multiple small areas (maximum diameter <2 mm on T_2 weighted sequences), distributed evenly inside the tumor were defined as having a "mosaic-like" appearance; and all other tumors not presenting the signal characteristics described above were defined as "solid"[17,18] ;

-*T_1W and T_2W SI (rSI)*: defined as the ratio between the solid portion of the lesion and the normal white matter visible on the same image, in the temporal lobe, identified in the baseline T_1- and T_2 weighted sequences; the methods for these analyzes have been described and validated elsewhere[19–21] ;

-*Degree of contrast uptake* (enhancement ratio – ER): obtained by calculating the ratio between the SI in T_1 weighted images after contrast administration and baseline T_1 weighted images in the solid portion of the adenoma;

Regions of interest (ROIs) for ER analysis were drawn directly on the images obtained with conventional sequences in the solid portion of the adenoma, avoiding areas of cystic or hemorrhagic degeneration. Similar ROIs were also identified in the normal white matter visible on the same image, in the temporal lobe in order to normalize the data obtained using an internal control.[8,9,14,16,19] All ROIs were of an arbitrarily chosen uniform

Figure 1. (a–c) ROIs placement on T_2W (a), T_2W (b) and T_1 +c (c) images both on solid component of a pituitary macroadenoma and on reference region (white matter of the left temporal pole). ROI, region of interest.

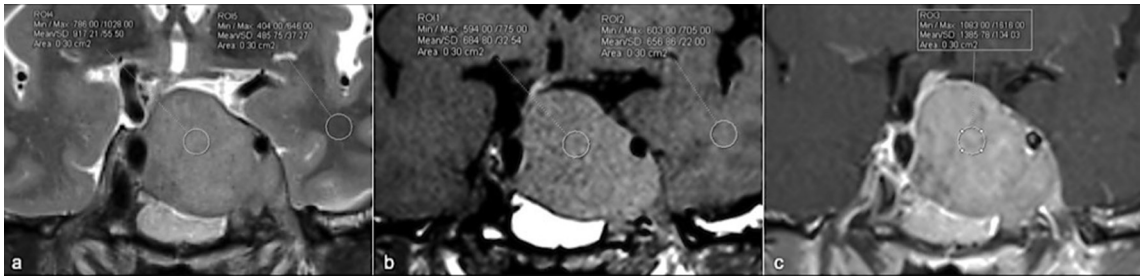

shape and size (elliptical ROIs of approximately 30–50 mm^2) (Figure 1).

DWI protocol and processing

The diffusion-weighted study targeted on the PA was performed using a high spatial resolution DWI sequence (values of b = 0–1.000 s/mm^2, TR = 3190 ms, TE1 = 64 ms, TE2 = 100 ms, fat saturation, FOV = 24×24 cm, matrix = 160×160, thickness/gap = 2/0 mm, Averages = 0–6) acquired on a bicommissural axial plane using a readout-segmented multishot echoplanar imaging (EPI) technique(*REadout Segmentation Of Long Variable Echo trains – syngo RESOLVE ® Siemens Healthcare*) using data from a two-dimensional navigator acquisition to perform a real-time motion artifact correction. The advantage of this technique over the more conventional single-shot EPI diffusion studies lies in the reduction in magnetic susceptibility artefacts and blurring even at high magnetic field intensities (3 T).[22]

The parametric maps obtained from the diffusion studies were processed by using a dedicated software of the MRI platform(*syngo.via ® - Siemens Healthineers*). The ADC maps were generated automatically by adapting a linear regression model to the logarithmic signal decrease at the different b-values applied.

To ensure precise ROI placement on the solid tumor component and avoid cystic, hemorrhagic and necrotic areas, the DWI images were co-registered with conventional MRI T_1W pre- and post-gadolinium and T_2W. Hence, the mean ADC values (ADCm) were measured by manually placing from three to five ROIs on the lower appearance ADC maps (Figure 2). The lower ADCm values for each patient were considered. Eventually, to minimize variances in ADCm values, relative ADC (rADC) was obtained from the ratios of the tumor ADCm to ADCm of a normal appearing reference region (white matter of the temporal lobe), defined on T_2W and contrast-enhanced T_1W.

Figure 2. (a–b) ROIs placement on co-registered T_1W + c (a) and ADC (b) images both on solid component of a PM and on white matter of the left temporal pole (as reference region). The lower mean ADC values were chosen. ADC, apparent diffusioncoefficient; PM, pituitary macroadenoma; ROI, region of interest.

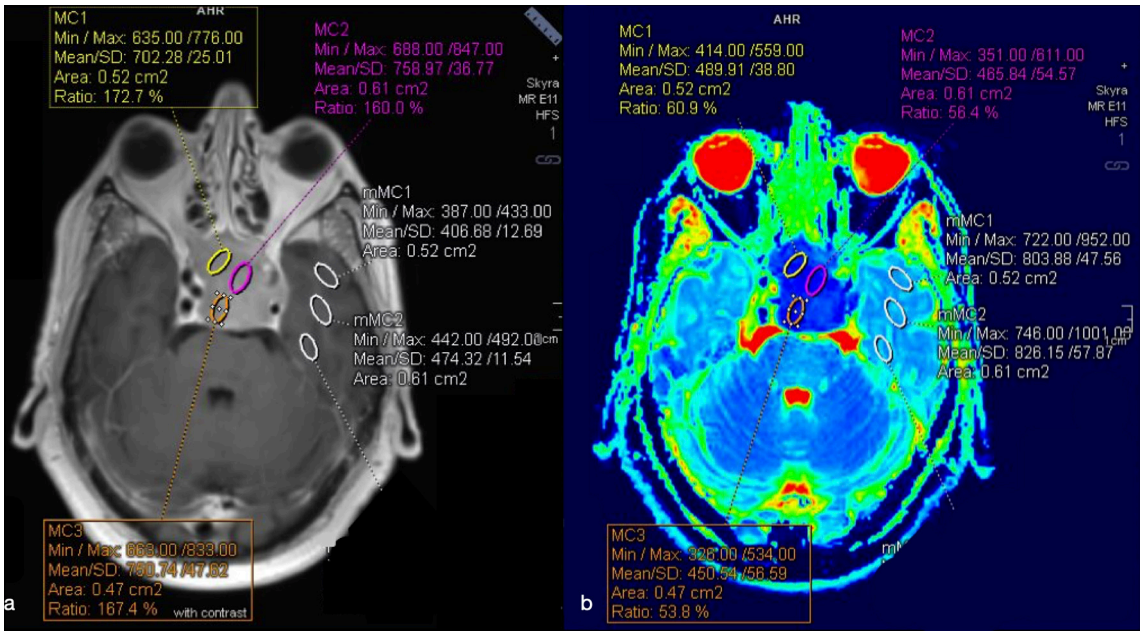

Histological analysis

The tumor samples were stained with H&E for routine analysis. According to the most recent edition of the WHO classification of tumors of endocrine organs,[6] the pathologist provided a diagnostic assessment of the lesion by using an immunohistochemical analysis of the main hormones and the pituitary transcription factors.

The Ki-67 LI was reported as the percentage of tumor cells with positive nuclei in the lesion areas with the greatest labelling density, known as hotspots, using high-power fields (HPF – 0.30 mm^2, 400x magnification). The mitotic count, on the other hand, was expressed as the number of mitotic figures/10 HPF.[7]

Clinicopathological classification

All the PM were subclassified using the principles proposed by Trouillas et al, taking into account radiological (Knosp grading system) and histological invasion criteria of the sphenoid sinus or cavernous sinuses. Moreover, the histopathological proliferation criteria were also considered. In particular, according the clinicopathological classification, proliferation criteria include the presence of at least two of the three among: Ki-67:≥1% (Bouin-Hollande fixative) or ≥3% (formalin fixative), Mitoses: $n \geq 2/10$ HPF and P53: positive (≥10 strongly positive nuclei/10 HPF).[2] Since not in all the cases immunohistochemical staining for p53 was performed, we considered as "proliferative" mocroadenomas which presented both Ki-67 LI ≥3% and a number of mitoses ≥ 2/10 HPF.

Thus, based on the analysis of radiological local tumor invasion and histopathological proliferation indices, the lesions were stratified into Grade 1a ("not-invasive and not-proliferative"; six lesions, 35.30%), Grade 1b ("not-invasive and proliferative"; one lesion, 5.88%), Grade 2a ("invasive and not-proliferative"; five lesions, 29.41%) and Grade 2b ("invasive and proliferative"; five lesions 29.41%). In our population, every PA with a value of Ki-67 LI ≥3% also presented a mitotic count ≥2/10 HPF.

Statistical analysis

The statistical analysis was performed using Stata 14.2 software. In the descriptive analysis, the continuous variables were summarized and expressed as median and interquartile ranges or mean and standard deviation (on the basis of distribution), and the categorical variables were expressed as absolute values and percentages.

Spearman's ρ was calculated to evaluate the correlation between the degree of Ki-67 LI of the PM and each of the quantitative values obtained from the MRI examination. A further correlation analysis between the same imaging data and the clinicopathological classification[2] was performed. Moreover, to identify any differences in ER, T_2WSI, T_1WSI and ADCm values between Grade 2b and the other groups the nonparametric Mann–Whitney test was used.

The receiver operating characteristic (ROC) was applied and logistic regression modelling were performed to determine the ability of ADCm to discriminate the PM with Ki67-LI ≥ 3% and the 2b group according the clinicopathological classification. The sensitivity, specificity and area under the curve based on optimum thresholds for variable parameters were calculated. A p-value ≤ 0.05 was considered statistically significant for all the tests.

Table 1. Magnetic Resonance and Histologic characteristics of the PMgeneral population

		Rate (%)
Sex (male/female)	12/5	70/30
Age	56.1 ± 10.0	
Volume (ml) – mean (RIQ)	16 (6 – 31)	
Signal intensity homogeneity	8	
Solid	10	58.82
Macrocistics	3	17.65
Mosaic-like	4	23.53
Knospgradindgsystem		
Grade 0–3	7	41.18
Grade 3–4	10	58.82
Adenoma Hystology		
Somatotroph	1	5.8
Lactotroph	1	5.8
Plurihormonal	1	5.8
Corticotroph	2	11.76
Gonadotroph	12	70.60
Ki-67 LI		
LI < 3%	11	64.71
LI ≥ 3%	6	35.29
Mitoticcount (n/10 HPF)		
<2/10 HPF	8	47.06
≥2/10 HPF	9	52.94
TrouillasClassification:		
1a	6	35.3
1b	1	5.8
2a	5	29.4
2b	5	29.4

RESULTS

Pathological and cMRI characteristics of the PM are summarized in the Table 1. In all patients, it was possible to perform the quantitative measurements of the T_1- and T_2 weighted images and of the ADCm parametric maps.

Both rSIT_2 and rSIT_1 showed no statistically significant correlations with Ki-67 LI nor with the clinicopathological classification proposed by Trouillas et al.[2]

Negative correlations were observed both between Ki-67 LI and ADCm ($p = 0.005$, $r = -0.67$)and Ki-67and ER values ($p = 0.008$,

Figure 3. Plot of ADCm values versus Ki67-LI demonstrates an inverse association between these parameters (p = 0.005, r = −0.67). The flat appearance of the correlation line is due to one outlier higher value (KI67-LI > 25%). ADC, apparent diffusioncoefficient; LI, labelling index.

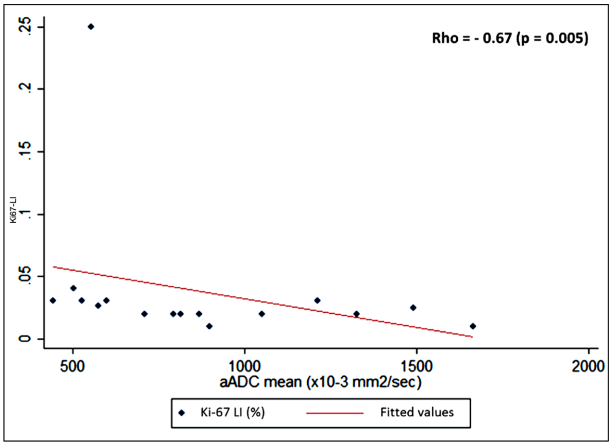

r = −0.62) (Figure 3). The ADCm and ER values were significantly lower in the group with values of Ki67-LI ≥ 3% (Table 2, Figure 4).A negative relationship was also detected between ADCm and the clinicopathological classification (r = −0.49; p = 0.05). Moreover, higher ADCm values were positively correlated with ER values (r = 0.60 p = 0.015).

The differences in rSIT_1, rSIT_1, ER and ADCm between the "2b" PM group and the other groups are summarized in the Table 3. In particular, ER values were lower in the 2bPM group if compared with the other groups (p = 0.028).

In the ROC analysis, a value of ADCm ≤0.711×10^{-6} mm^2/s emerged as a cut-off of Ki67-LI ≥ 3% and 2b macroadenomas group according the Trouillas's classification. In particular, ADCm showed sensitivity and specificity of 90 and 85% respectively (AUC value: 0,866) in differentiating the Ki67-LI ≥ 3% PM group and a sensitivity and specificity of 81 and 80% respectively (AUC value: 0,800) in differentiating the 2b group according the clinicopathological classification.

DISCUSSION

The aim of the study was to evaluate the role of cMRI and ADC maps in order to establish biomarkers able to identify the likely PM with aggressive behavior. Indeed, although they are "benign" from a histological standpoint, PM present a vast range of biological behavior, and, in some cases, can present rapid growth, with the invasion of the adjacent structures, and early relapse after treatment.[2–5]

As expected, we observed the existence of a negative correlation between Ki-67 LI and ADC values (r = - 0.67, p-value 0.005) (Figure 3). These results are consistent with those recently reported in the study by Tamrazi et al.[13] In particular, the ADCm values were significantly lower in the group of macroadenomas characterized by a Ki-67 LI value ≥3% than the group of PM with Ki-67 LI <3% (p-value 0.017).

On the other hand, both rSIT_2 and rSIT_1 showed no statistically significant correlations with PM proliferative index.

These findings suggest that diffusion techniques have the capability to characterize PM better than cMRI sequences alone, as they are able to provide an objective parameter (ADC) as a radiological biomarker suggestive of high proliferative activity.

Establishing the biological aggressiveness of PM is essential for both an appropriate surgical resection and long-term follow-up, especially in presence of a residual lesion after treatment. As well-known, cMRI is able to determine the likelihood of cavernous sinuses invasion by PA[1,15,16] although it does not provide any meaningful information regarding their proliferative potential. Indeed, multiple factors can affect PM signal intensity on cMRI sequences, thus limiting their diagnostic utility in this specific context. This is probably due to the fact that PM signal intensity, especially on T_2 weighted images, has been related to different biological features of the tumor, such as its fibrous or microcystic content, as well as the tumor cellularity[18] and its hormonal secretory activity.[23] However, the recent introduction of machine learning or radiomics analysis of texture-derived parameters from T_2-weighted images applied to PM, has proven to be effective for the preoperative prediction of both KI-67 LI and tumor consistency.[24,25] These studies suggested that the limitations of T_2 weighted images alone could be solved in the future.

Table 2. Differences in rSI T1, rSI T2, ER and ADCm between Ki67-IL groups (cut-off ≥ *3%)*. Significant differences (*) were find in ADCm and ER values.

Ki-67 LI	*< 3%*	*≥ 3%*	*p-value*
rSI T1	1.11 (1.07 – 1.16)	1.08 (1.02 – 1.11)	0.207
rSI T2	2.11 (1.71 – 2.18)	1.82 (1.26 – 2.26)	0.366
ER	2.14 (1.98 – 2.29)	1.86 (1.62 – 1.92)	*0.012
ADCm	0.884 (0.793 – 1.327)	0.542(0.504 – 0.599)	*0.017
rADCm	1.07 (1.00 – 1.63)	0.67 (0.64 – 0.81)	*0.017

ADCm, mean apparent diffusion coefficient (x 10^{-6} mm^2/sec); ER, enhancement ratio; Ki-67 LI, Ki-67 labelling index; rADCm, relative mean ADC; rSI T1, signal intensity ratio T1-weighted images; rSI T2, signal intensity ratio T2-weighted images.

Figure 4. Enhancement ratio (a) and ADCm (b)differences between KI67-LI groups. On each box, the horizontal line is the median and the edges of the box are the 25th and 75th percentiles. Both ER (p = 0.012) and ADCm (p = 0.017) values were lower in the PM group with Ki67-LI ≥ 3%. ADC, apparent diffusioncoefficient; LI, labelling index; PM, pituitary macroadenoma

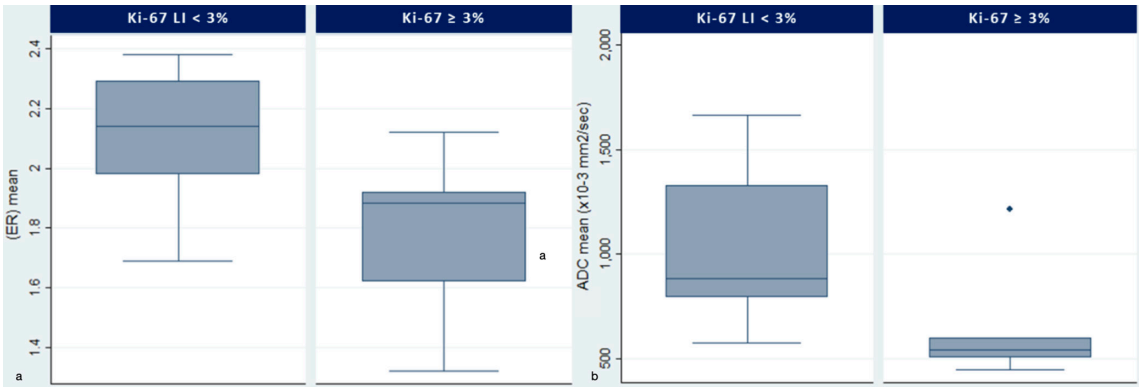

On the other hand, DWI is able to further characterize PM, delineating lesions that cannot be otherwise identified with conventional studies. Moreover, in our patient sample, ADCm values were negatively related also with the clinicopathological classification (r = −0.49; p = 0.05), reflecting a more complex patients' subdivision. Indeed, a value of ADCm ≤0.711×10^{-6} mm^2/s could be considered a "cut-off" of both Ki-67LI ≥ 3% values and 2b (invasive and proliferative) group according the Trouillas classification.[2]

Thus, the use of ADC allows to recognize PM with histopathological features related to a high proliferative activity and to a high probability of recurrence,[7] regardless of their invasive behavior.

In the past, a number of studies have identified a more or less consistent correlation between Ki-67 LI and ADC values in various tumor types and a recent meta-analysis showed that they would appear to be strongest in ovarian tumors, urothelial cancer, lung cancer, cerebral lymphoma and neuroendocrine tumors.[12] Although a number of different factors would appear to play a role, the exact biological rationale underlying this association is not completely clear. Ki-67 LI is a nuclear non-histone protein involved in cell proliferation processes.[26] Given its associations with nucleus cell size (which increases during the mitotic phase of the cell cycle[11,26]), and with the cellularity and histological grade in various types of tumor,[27–32] it is therefore plausible that the ADC value may reflect the proliferative activity of PM, thus representing an added value of DWI compared to cMRI sequences.

Among the cMRI sequences, the only factor associated with the PM proliferative index was the ER; indeed, it was negatively correlated to Ki-67 LI (p = 0.008).

In our analysis, the 2b PM group, according the clinicopathological classification, showed ER values (p = 0.028) lower than other PM groups. Hence, MRI is potentially able to predict the clinicopathological grading, further stratifying invasive macroadenomas into two groups characterized by a different proliferative capacity and prognosis.

The lower ER values we detected in this group could explain the intratumoral microvessels organization of the pituitary gland and PM. Indeed, although increased angiogenesis has been detected to correlated with tumor growth and metastatic potential in many different tumor types,[33] PM have significantly lower vascular densities as compared to non-tumoros adenohypophysis.[34,35]

Furthermore, recently has been reported that the perfusion fraction in PM is significantly lower than that in normal pituitary

Table 3. Differences in rSI T1, rSI T2, ER and ADCm between "invasive and proliferative" vs other PM groups. Significant differences (*) were detected in ADCm and ER values.

Clinicopathologicalclassification	*Othergroups(Grade 1a,1b,2a)*	*Invasive and Proliferative(2b)*	*p*-value
rSI T1	1.07 (1.07–1.09)	1.06 (1.02–1.10)	0.600
rSI T2	2.15 (1.93–2.18)	1.89 (1.75–2.26)	0.602
ER	2.14 (1.98–2.29)	1.92 (1.85–1.92)	*0.028
ADCm	0.869 (0.793–1.051)	556.14 (504.92–599.91)	0.117
rADCm	1.05 (1.00–1.08)	0.67 (0.64–0.81)	0.117

ADCm, mean apparent diffusion coefficient (x 10^{-6} mm^2/sec); ER, enhancement ratio; Ki-67 LI, Ki-67 labelling index; rADCm, relative mean ADC; rSI T1, signal intensity ratio T1-weighted images; rSI T2, signal intensity ratio T2-weighted images.

glands and it was attributed to the lower microvessel area in PM compared to normal pituitary glands.[36]

Moreover, interestingly a study regarding microvascular structural entropy[37] detected that regular, less chaotic microvascular geometry contributes to increased proliferative activity in PA producing prolactin.

Lastly, we found that higher ADCm values were positively correlated with ER values (r = 0.60 p = 0.015) in the overall group. The restricted ADC observed in many malignant tissues can be attributed to their higher cellular structures than benign and normal tissues.[11,38] This leads to an increase in volume of the intracellular space, at the expense of the extracellular one. Moreover, the extracellular space has a higher water content than the intracellular one, therefore it can be deduced that lesions with low Ki-67 LI have a greater extracellular space containing the abnormal vessels, responsible for the greater enhancement of the lesions.

We believe that our finding concerning ER, can adequately reflect the structural characteristics of this type of tumors. Moreover, ER may not be considered as a predictive parameter of aggression, as occurs for brain metastases and high grade tumor. Hence, analysis of vascularization has no value in predicting tumor growth of PM.

LIMITATIONS

The main limit of this study is the small patient sample size examined in this preliminary study phase. Nevertheless, it was possible to observe a number of significant associations between the data obtained from pre-operative MRI, and the PA proliferative activity. Despite the limited size of the analyzed sample, it is worth noting the good inverse correlation between the ADC and Ki-67 LI values, identifying DWI as a biomarker predictive of the proliferative activity of PM.

However, prospective studies with larger patient samples such as multicenter studies with different MRI equipment are needed to confirm these results and to validate this method.

Moreover, it should be taken into account that the surgical sample available to the pathologist varies greatly and may not be representative of the tumor as a whole. This aspect could also influence the Ki-67 LI assessment, especially in macroadenomas with a nonhomogeneous structure, thereby limiting the subsequent analysis of the association and correlation with the variables analyzed in the pre-operative MRI.

Lastly, the simplified description of the diffusion process assumed in DWI sequences does not permit to completely map the complexity underlying cellular components and structures, which hinder and restrict the diffusion of water molecules. Indeed, ADC values are affected by both molecular diffusion and blood perfusion, so they do not represent true tissue characteristics. Thus, the use of more advanced MRI pulse sequences and a higher order of diffusion model (*e.g.* through the use of multiple b values for intravoxel incoherent motion analyzes, which can separate the perfusion components from the true diffusion of water molecules, allowing the quantification of the true diffusion coefficient, the pseudodiffusion coefficient, and the perfusion fraction) may partially overcome these limits at the cost of less user-friendly and more time-consuming pre- and post-processing workflows.[39]

CONCLUSIONS

Establishing the biological PM's aggressiveness is important for both an appropriate surgical resection and the long-term follow-up of these patients, especially in presence of a residual lesion after treatment. Despite being necessary in order to establish the extent of the tumor and any invasion of the adjacent structures, conventional imaging is unable to provide this information. Modern diffusion imaging techniques are now able to provide high-definition images that are sufficiently reliable even in the sellar and parasellar regions, thereby adding a further characterization approach that should be included in the routine pre-operative study of pituitary adenomas. Future studies with larger sample sizes are needed to improve statistical power and verify these observations. Lastly, studies on machine learning analysis of texture-derived parameters from pre-operative DWI could make a more accurate lesion classification and allow for a more focused follow-up and long-term management.

COMPETING INTERESTS

The authors declare that they have no conflicts of interest neither competing interests.

FUNDING

The authors declare that no source of funding has served to conduct the research.

ETHICS APPROVAL

Etic Committee: Area Vasta Centro, Bologna, protocol: PIT-MRI-201

REFERENCES

1. JL G. Rajamohan Ag.: imaging of the sella and Parasellar region. *Radiol Clin North Am* 2017; **55**: 83–01.
2. Trouillas J, Roy P, Sturm N, Dantony E, Cortet-Rudelli C, Viennet G, et al. A new prognostic clinicopathological classification of pituitary adenomas: a multicentric case-control study of 410 patients with 8 years post-operative follow-up. *Acta Neuropathol* 2013; **126**: 123–35. doi: https://doi.org/10.1007/s00401-013-1084-y
3. Chatzellis E, Alexandraki KI, Androulakis II, Kaltsas G. Aggressive pituitary tumors.

Neuroendocrinology 2015; **101**: 87–104. doi: https://doi.org/10.1159/000371806
4. Scheithauer BW, Gaffey TA, Lloyd RV, Sebo TJ, Kovacs KT, Horvath E, et al. Pathobiology of pituitary adenomas and carcinomas. *Neurosurgery* 2006; **59**: 341–53. doi: https://doi.org/10.1227/01.NEU.0000223437.51435.6E
5. Asioli S, Righi A, Iommi M, Baldovini C, Ambrosi F, Guaraldi F, et al. Validation of a clinicopathological score for the prediction of post-surgical evolution of pituitary adenoma: retrospective analysis on 566 patients from a tertiary care centre. *Eur J Endocrinol* 2019; **180**: 127–34. doi: https://doi.org/10.1530/EJE-18-0749
6. Osamura RY, Grossman A, Korbonits M, Kovacs K, Lopes MBS. Matsuno A & Trouillas J.: Pituitary adenoma. In: Lloyd R. V, Osamura R. Y, Kloppel G, Rosai J, eds.*World Health Organization Classification of Tumours of Endocrine Organs*. 4th ed.. Lyon: IARC; 2017. pp. 14–18.
7. Lopes MBS, The LMBS. The 2017 World Health organization classification of tumors of the pituitary gland: a summary. *Acta Neuropathol* 2017; **134**: 521–35. doi: https://doi.org/10.1007/s00401-017-1769-8
8. Pierallini A, Caramia F, Falcone C, Tinelli E, Paonessa A, Ciddio AB, et al. Pituitary macroadenomas: preoperative evaluation of consistency with diffusion-weighted MR imaging--initial experience. *Radiology* 2006; **239**: 223–31. doi: https://doi.org/10.1148/radiol.2383042204
9. Mahmoud OM, Tominaga A, Amatya VJ, Ohtaki M, Sugiyama K, Sakoguchi T, et al. Role of propeller diffusion-weighted imaging and apparent diffusion coefficient in the evaluation of pituitary adenomas. *Eur J Radiol* 2011; **80**: 412–7. doi: https://doi.org/10.1016/j.ejrad.2010.05.023
10. Kwee TC, Takahara T, Ochiai R, Katahira K, Van Cauteren M, Imai Y, et al. Whole-Body diffusion-weighted magnetic resonance imaging. *Eur J Radiol* 2009; **70**: 409–17. doi: https://doi.org/10.1016/j.ejrad.2009.03.054
11. Padhani AR, Koh D-M, Collins DJ. Whole-Body diffusion-weighted MR imaging in cancer: current status and research directions. *Radiology* 2011; **261**: 700–18. doi: https://doi.org/10.1148/radiol.11110474
12. Surov A, Meyer HJ, Wienke A. Correlation between apparent diffusion coefficient (ADC) and cellularity is different in several tumors: a meta-analysis. *Oncotarget* 2017; **8**: 59492–9. doi: https://doi.org/10.18632/oncotarget.17752
13. Tamrazi B, Pekmezci M, Aboian M, Tihan T, Glastonbury CM. Apparent diffusion coefficient and pituitary macroadenomas: pre-operative assessment of tumor atypia. *Pituitary* 2017; **20**: 195–200. doi: https://doi.org/10.1007/s11102-016-0759-5
14. Drake-Pérez M, Smirniotopoulos JG. Extraparenchymal lesions in adults. *Neuroimaging Clin N Am* 2016; **26**: 621–46. doi: https://doi.org/10.1016/j.nic.2016.06.009
15. Knosp E, Steiner E, Kitz K, Matula C. Pituitary adenomas with invasion of the cavernous sinus space: a magnetic resonance imaging classification compared with surgical findings. *Neurosurgery* 2013; **33**: 610–7.
16. Cottier JP, Destrieux C, Brunereau L, Bertrand P, Moreau L, Jan M, et al. Cavernous sinus invasion by pituitary adenoma: MR imaging. *Radiology* 2000; **215**: 463–9. doi: https://doi.org/10.1148/radiology.215.2.r00ap18463
17. Yamamoto J, Kakeda S, Shimajiri S, Takahashi M, Watanabe K, Kai Y, et al. Tumor consistency of pituitary macroadenomas: predictive analysis on the basis of imaging features with contrast-enhanced 3D FIESTA at 3T. *AJNR Am J Neuroradiol* 2014; **35**: 297–303. doi: https://doi.org/10.3174/ajnr.A3667
18. Boxerman JL, Rogg JM, Donahue JE, Machan JT, Goldman MA, Doberstein CE. Preoperative MRI evaluation of pituitary macroadenoma: imaging features predictive of successful transsphenoidal surgery. *AJR Am J Roentgenol* 2010; **195**: 720–8. doi: https://doi.org/10.2214/AJR.09.4128
19. Potorac I, Petrossians P, Daly AF, Schillo F, Ben Slama C, Nagi S, et al. Pituitary MRI characteristics in 297 acromegaly patients based on T2-weighted sequences. *Endocr Relat Cancer* 2015; **22**: 169–77. doi: https://doi.org/10.1530/ERC-14-0305
20. Potorac I, Petrossians P, Daly AF, Alexopoulou O, Borot S, Sahnoun-Fathallah M, et al. T2-Weighted MRI signal predicts hormone and tumor responses to somatostatin analogs in acromegaly. *Endocr Relat Cancer* 2016; **23**: 871–81. doi: https://doi.org/10.1530/ERC-16-0356
21. Heck A, Emblem KE, Casar-Borota O, Bollerslev J, Ringstad G. Quantitative analyses of T2-weighted MRI as a potential marker for response to somatostatin analogs in newly diagnosed acromegaly. *Endocrine* 2016; **52**: 333–43. doi: https://doi.org/10.1007/s12020-015-0766-8
22. Porter DA, Heidemann RM. High resolution diffusion-weighted imaging using readout-segmented echo-planar imaging, parallel imaging and a two-dimensional navigator-based reacquisition. *Magn Reson Med* 2009; **62**: 468–75. doi: https://doi.org/10.1002/mrm.22024
23. Yiping L, Ji X, Daoying G, Bo Y. Prediction of the consistency of pituitary adenoma: a comparative study on diffusion-weighted imaging and pathological results. *J Neuroradiol* 2016; **43**: 186–94. doi: https://doi.org/10.1016/j.neurad.2015.09.003
24. Ugga L, Cuocolo R, Solari D, Guadagno E, D'Amico A, Somma T, et al. Prediction of high proliferative index in pituitary macroadenomas using MRI-based radiomics and machine learning. *Neuroradiology* 2019; **61**: 1365–73. doi: https://doi.org/10.1007/s00234-019-02266-1
25. Zeynalova A, Kocak B, Durmaz ES, Comunoglu N, Ozcan K, Ozcan G, et al. Preoperative evaluation of tumour consistency in pituitary macroadenomas: a machine learning-based histogram analysis on conventional T2-weighted MRI. *Neuroradiology* 2019; **61**: 767–74. doi: https://doi.org/10.1007/s00234-019-02211-2
26. Schlüter C, Duchrow M, Wohlenberg C, Becker MH, Key G, Flad HD, et al. The cell proliferation-associated antigen of antibody Ki-67: a very large, ubiquitous nuclear protein with numerous repeated elements, representing a new kind of cell cycle-maintaining proteins. *J Cell Biol* 1993; **123**: 513–22. doi: https://doi.org/10.1083/jcb.123.3.513
27. Catalaa I, Henry R, Dillon WP, Graves EE, McKnight TR, Lu Y, et al. Perfusion, diffusion and spectroscopy values in newly diagnosed cerebral gliomas. *NMR Biomed* 2006; **19**: 463–75. doi: https://doi.org/10.1002/nbm.1059
28. Manenti G, Di Roma M, Mancino S, Bartolucci DA, Palmieri G, Mastrangeli R, et al. Malignant renal neoplasms: correlation between ADC values and cellularity in diffusion weighted magnetic resonance imaging at 3 T. *Radiol Med* 2008; **113**: 199–213. doi: https://doi.org/10.1007/s11547-008-0246-9
29. Hayashida Y, Hirai T, Morishita S, Kitajima M, Murakami R, Korogi Y, et al. Diffusion-Weighted imaging of metastatic brain tumors: comparison with histologic type and tumor cellularity. *AJNR Am J Neuroradiol* 2006; **27**: 1419–25.
30. Humphries PD, Sebire NJ, Siegel MJ, Olsen Øystein E, Olsen OE. Tumors in pediatric patients at diffusion-weighted MR imaging: apparent diffusion coefficient and tumor cellularity. *Radiology* 2007; **245**: 848–54. doi: https://doi.org/10.1148/radiol.2452061535
31. Zelhof B, Pickles M, Liney G, Gibbs P, Rodrigues G, Kraus S, et al. Correlation of diffusion-weighted magnetic resonance data with cellularity in prostate cancer. *BJU Int*

2009; **103**: 883–8. doi: https://doi.org/10.1111/j.1464-410X.2008.08130.x

32. Liu Y, Bai R, Sun H, Liu H, Wang D. Diffusion-Weighted magnetic resonance imaging of uterine cervical cancer. *J Comput Assist Tomogr* 2009; **33**: 858–62. doi: https://doi.org/10.1097/RCT.0b013e31819e93af
33. García-Figueiras R, Padhani AR, Beer AJ, Baleato-González S, Vilanova JC, Luna A, et al. Imaging of Tumor Angiogenesis for Radiologists--Part 1: Biological and Technical Basis. *Curr Probl Diagn Radiol* 2015; **44**: 407–24. doi: https://doi.org/10.1067/j.cpradiol.2015.02.010
34. Turner HE, Nagy Z, Gatter KC, Esiri MM, Harris AL, Wass JA. Angiogenesis in pituitary adenomas and the normal pituitary gland. *J Clin Endocrinol Metab* 2000; **85**: 1159–62. doi: https://doi.org/10.1210/jcem.85.3.6485
35. Yamada S, Takada K. Angiognesis in pituitary adenomas microscopy research and technique. *Microsc Res Tech* 2003; **60**: 236–43.
36. Kamimura K, Nakajo M, Yoneyama T, Fukukura Y, Fujio S, Goto Y, et al. Assessment of microvessel perfusion of pituitary adenomas: a feasibility study using turbo spin-echo-based intravoxel incoherent motion imaging. *Eur Radiol* 2020; **30**: 1908–17. doi: https://doi.org/10.1007/s00330-019-06443-x
37. Vidal S, Horvath E, Kovacs K, Lloyd RV, Scheithauer BW. Microvascular structural entropy: a novel approach to assess angiogenesis in pituitary tumors. *Endocr Pathol* 2003; **14**: 239–47. doi: https://doi.org/10.1007/s12022-003-0016-0
38. Hobbs SK, Shi G, Homer R, Harsh G, Atlas SW, Bednarski MD. Magnetic resonance image-guided proteomics of human glioblastoma multiforme. *J Magn Reson Imaging* 2003; **18**: 530–6. doi: https://doi.org/10.1002/jmri.10395
39. Wu W-C, Yang S-C, Chen Y-F, Tseng H-M, My P-C, WC W, PC M. Simultaneous assessment of cerebral blood volume and diffusion heterogeneity using hybrid IVIM and DK MR imaging: initial experience with brain tumors. *Eur Radiol* 2017; **27**: 306–14. doi: https://doi.org/10.1007/s00330-016-4272-z